AD-A137 544 UNCOUPLING APPROXIMATION FOR THE DYNAMIC ANALYSIS OF STRUCTURES EMBEDDED I..(U) WEIDLINGER ASSOCIATES NEW YORK J P WRIGHT ET AL. 01 JUL 80 DNA-5396T 1/1

UNCLASSIFIED DNA001-79-C-0227 F/G 13/13 NL

END
FILMED
3-84
DTIC

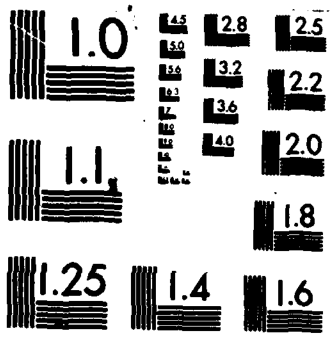

MICROCOPY RESOLUTION TEST CHART
NATIONAL BUREAU OF STANDARDS-1963-A

AD-E301320

(12)

DNA 5396T

ADA137544

UNCOUPLING APPROXIMATION FOR THE DYNAMIC ANALYSIS OF STRUCTURES EMBEDDED IN HYSTERETIC MEDIA

Weidlinger Associates, Consulting Engineers
333 Seventh Avenue
New York, New York 10001

1 July 1980

Topical Report

CONTRACT No. DNA 001-79-C-0227
and
CONTRACT No. DNA 001-79-C-0256

APPROVED FOR PUBLIC RELEASE;
DISTRIBUTION UNLIMITED.

THIS WORK WAS SPONSORED BY THE DEFENSE NUCLEAR AGENCY UNDER RDT&E RMSS CODES B344079464 Y99QAXSC06169 H2590D AND B344079464 Y99QAXSC37020 H2590D.

Prepared for
Director
DEFENSE NUCLEAR AGENCY
Washington, DC 20305

Destroy this report when it is no longer needed. Do not return to sender.

PLEASE NOTIFY THE DEFENSE NUCLEAR AGENCY, ATTN: STTI, WASHINGTON, D.C. 20305, IF YOUR ADDRESS IS INCORRECT, IF YOU WISH TO BE DELETED FROM THE DISTRIBUTION LIST, OR IF THE ADDRESSEE IS NO LONGER EMPLOYED BY YOUR ORGANIZATION.

UNCLASSIFIED

SECURITY CLASSIFICATION OF THIS PAGE (When Data Entered)

REPORT DOCUMENTATION PAGE		READ INSTRUCTIONS BEFORE COMPLETING FORM
1. REPORT NUMBER DNA 5396T	2. GOVT ACCESSION NO. AD-A137544	3. RECIPIENT'S CATALOG NUMBER
4. TITLE (and Subtitle) UNCOUPLING APPROXIMATION FOR THE DYNAMIC ANALYSIS OF STRUCTURES EMBEDDED IN HYSTERETIC MEDIA		5. TYPE OF REPORT & PERIOD COVERED Topical Report for Period 1 Jan 79—1 Jul 80 6. PERFORMING ORG. REPORT NUMBER
7. AUTHOR(s) Joseph P. Wright Robert Smilowitz		8. CONTRACT OR GRANT NUMBER(s) DNA 001-79-C-0227 and DNA 001-79-C-0256
9. PERFORMING ORGANIZATION NAME AND ADDRESS Weidlinger Associates, Consulting Engineers 333 Seventh Avenue New York, New York 10001		10. PROGRAM ELEMENT, PROJECT, TASK AREA & WORK UNIT NUMBERS Subtasks Y99QAXSC061-69 and Y99QAXSC370-20
11. CONTROLLING OFFICE NAME AND ADDRESS Director Defense Nuclear Agency Washington, DC 20305		12. REPORT DATE 1 July 1980 13. NUMBER OF PAGES 42
14. MONITORING AGENCY NAME & ADDRESS(if different from Controlling Office)		15. SECURITY CLASS (of this report) UNCLASSIFIED 15a. DECLASSIFICATION/DOWNGRADING SCHEDULE N/A since UNCLASSIFIED

16. DISTRIBUTION STATEMENT (of this Report)

Approved for public release; distribution unlimited.

17. DISTRIBUTION STATEMENT (of the abstract entered in Block 20, if different from Report)

18. SUPPLEMENTARY NOTES

This work was sponsored by the Defense Nuclear Agency under RDT&E RMSS Codes B344079464 Y99QAXSC06169 H2590D and B344079464 Y99QAXSC37020 H2590D.

19. KEY WORDS (Continue on reverse side if necessary and identify by block number)

Wave Propagation
Soil-Structure Interaction
Radiation Damping
Protective Structures

20. ABSTRACT (Continue on reverse side if necessary and identify by block number)

The main purpose of this study is to consider an uncoupling method for analyzing explosively loaded structures embedded in hysteretic media. The method, which is based on wave propagation considerations, can be viewed as the plane wave approximation extended to nonlinear problems. Free-field data (both traction and velocity vectors) must be known in order to apply the method. Accuracy of the approximation is shown to be quite good when applied to a series of one-dimensional soil-structure interaction problems, even when

DD FORM 1 JAN 73 1473 EDITION OF 1 NOV 65 IS OBSOLETE

UNCLASSIFIED

SECURITY CLASSIFICATION OF THIS PAGE (When Data Entered)

20. ABSTRACT (Continued)

the structure and surrounding soil are both nonlinear. Multi-dimensional problems, and techniques for improving the method, are also discussed briefly.

TABLE OF CONTENTS

LIST OF ILLUSTRATIONS

LIST OF ILLUSTRATIONS (Concluded)

1. INTRODUCTION

The dynamic response of buried structures subjected to explosive loadings can be analyzed using many different models. These range from simple models that involve a few parameters to extremely complicated models that represent many details of the explosion process, the surrounding ground materials, and the structure itself. The difficulties and uncertainties associated with simultaneously analyzing the explosion, the ground, and the structure usually lead to consideration of procedures that allow detailed study of some parts of the problem while treating the rest in a simplified fashion. Approximate procedures of this type will be referred to as uncoupling methods.

The main purpose of this study is to consider an uncoupling method that permits detailed analysis of the structure while the ground, which may exhibit hysteretic behavior, is represented by a relatively simple model based on an extension of the plane wave approximation. This method is a special case of a more general approach (currently under development by Weidlinger Associates, and is summarized in the Appendix) to uncouple the motion of a structure from that of a nonlinear medium with which it is in contact.

The plane wave approximation has been used as an uncoupling method for linear fluid-structure interaction problems for many years (e.g. see Ref. [2]). Recently, Ref. [3], it has been applied to the nonlinear problem of a structure submerged in a cavitating fluid. It has also played a role - in the form of viscous dampers - in the development of "transmitting" boundaries for soil-structure interaction calculations (both linear and nonlinear); here however the boundary is placed relatively far from the structure. Its application as a soil-structure uncoupling method, wherein the soil is entirely replaced by the plane wave approximation at the soil-structure interface, appears to be quite recent. It was successfully applied in this way to a linear two-dimensional problem in Ref. [4] and to a nonlinear two-dimensional situation in Ref. [5].

2. ONE DIMENSIONAL SOIL-STRUCTURE INTERACTION

Consider the soil-structure interaction problem illustrated in Fig. 1. A possible one dimensional model of the roof of the structure in contact with the soil is shown in Fig. 2. This one dimensional problem will be taken as the model with which the uncoupling method will be compared in detail.

2.1 Formulation of the Continuum Equations (see Fig. 2)

The soil, having density ρ_1 and depth H_1, is represented by piecewise linear stress-strain behavior with initial loading modulus M_L, and unload-reloading modulus M_U, where $M_U \geq M_L$. The structure, having density ρ_2 and depth H_2, is represented by a linear elastic stress-strain behavior with modulus M_2. The shearing resistance of the roof is represented by an elastic, ideally plastic continuous support that exerts a force F_S where the elastic force-displacement behavior is represented by a spring constant K and the plastic limit is represented by a force F_o.

Let x denote a coordinate, increasing with depth, with x = 0 corresponding to the ground surface. Let u(x,t) be the particle displacement at point x at time t in the continua, and $v(x, t) = \frac{\partial u}{\partial t}$ be the corresponding particle velocity. The stress, negative in compression, is denoted by $\sigma(x, t)$. Ignoring convective effects, the continuum equations for the soil can be written as

$$\rho_1 \frac{\partial v}{\partial t} = \frac{\partial \sigma}{\partial x} \tag{1}$$

$$\frac{\partial \sigma}{\partial t} = M_1 \frac{\partial v}{\partial x} \tag{2}$$

where M_1 is either M_L or M_U, depending on the state of the material. The continuum equations for the structure can be written as

$$\rho_2 \frac{\partial v}{\partial t} = \frac{\partial \sigma}{\partial x} + \frac{F_S}{H_2 A} \tag{3}$$

$$\frac{\partial \sigma}{\partial t} = M_2 \frac{\partial v}{\partial x} \tag{4}$$

where F_S depends on the state of the shear support, and A is the area of the structure that is in contact with the soil.

2.2 Finite Difference Equations

Equations 1 to 4 are solved numerically by finite differences using central differences in space and time on a staggered grid of stress and velocity points, as shown in Fig. 3. Stress points are placed at $x = 0$ and $x = (H_1 + H_2)$ and a velocity point is placed at $x = H_1$. In the soil region difference equations are expressed in terms of the length $\Delta x_1 = H_1/(N_1 + 1/2)$ where N_1 is an arbitrary positive integer. Similarly in the structure the difference equations are expressed in terms of the length $\Delta x_2 = H_2/(N_2 + 1/2)$ Let σ_i denote $\sigma(x_i, t)$ where $x_i = (i-1)\Delta x_1$ for $i = 1, 2, \ldots, N_1 + 1$ and $x_i = H_1 + (i - N_1 - 3/2)\Delta x_2$ for $i = N_1 + 2, \ldots, N_1 + N_2 + 2$. Let v_i denote $v(x_i, t)$ where $x_i = (i - 1/2)\Delta x_1$ for $i = 1, 2, \ldots, N_1 + 1$ and $x_i = H_1 +$ $(i - N_1 - 1)\Delta x_2$ for $i = N_1 + 2, \ldots, N_1 + N_2 + 1$. Difference approximations to Eqs. 1 and 2 can then be written as

$$v_i^{n+1} = \hat{v}_i^n + \frac{\Delta t}{\rho_1 \Delta x_1} (\sigma_{i+1}^n - \sigma_i^n) \quad \text{for } i = 1, 2, \ldots, N_1 \tag{5}$$

$$\sigma_i^{n+1} = \sigma_i^n + \frac{M_1 \Delta t}{\Delta x_1} (v_i^{n+1} - v_{i-1}^{n+1}) \quad \text{for } i = 2, \ldots, N_1 + 1 \tag{6}$$

where the superscripts denote time t_n or t_{n+1} and $\Delta t = t_{n+1} - t_n$ is the time increment.

The symbol $\hat{v}_i^n$ in Eq. 5 denotes a spatially averaged particle velocity, defined by

$$\hat{v}_i^n = v_i^n + \alpha_{i+1/2} (v_{i+1}^n - v_i^n) - \alpha_{i-1/2} (v_i^n - v_{i-1}^n) \qquad (7)$$

where every α must be non-negative. Small positive values of α introduce a linear (artificial) viscosity which can be used to suppress spurious high-frequency oscillations that are produced by this numerical method.

Similarly, difference approximations to Eqs. 3 and 4 can be written as

$$v_i^{n+1} = \hat{v}_i^n + \frac{\Delta t}{\rho_2 \Delta x_2} (\sigma_{i+1}^n - \sigma_i^n) + \frac{\Delta t}{\rho_2 H_2 A} F_{S,i}^n$$

$$\text{for } i = N_1 + 2, \ldots, N_1 + N_2 + 1 \qquad (8)$$

$$\sigma_i^{n+1} = \sigma_i^n + \frac{M_2 \Delta t}{\Delta x_2} (v_i^{n+1} - v_{i-1}^{n+1})$$

$$\text{for } i = N_1 + 2, \ldots, N_1 + N_2 + 2 \qquad (9)$$

where $F_{S,i}^n$ indicates that the displacement u_i^n is used in the force-displacement relation $F_S = -Ku$ of the shear support unless the plastic limit F_o controls. From the boundary conditions

$$\sigma_1^n = - P(t_n) \qquad (10)$$

where P(t) is the pressure loading at x = 0; at the free surface, $x = (H_1 + H_2)$

$$\sigma_{N_1+N_2+2}^n = 0 \qquad (11)$$

The velocity at the soil-structure interface is handled separately by

$$v_i^{n+1} = \hat{v}_i^n + \frac{\Delta t}{\bar{m}} (\sigma_{i+1}^n - \sigma_i^n) + \frac{\Delta t \Delta x_2}{2\bar{m} H_2 A} F_{S,i}^n$$

$$\text{for } i = N_1 + 1 \qquad (12)$$

where $\bar{m} = (\rho_1 \Delta x_1 + \rho_2 \Delta x_2)/2$.

2.3 Parametric Studies

The primary set of parameters for this model are

Geometry: H_1, H_2

Soil properties: ρ_1, M_L, M_U

Structural properties: ρ_2, M_2

Shear support: K, F_o

In this report the soil parameters will be given in terms of the loading wave speed

$$C_L = (M_L/\rho_1)^{1/2} \tag{13}$$

and the ratio of soil unloading modulus to loading modulus

$$U_o = M_U/M_L \geq 1 \tag{14}$$

Similarly the structural parameters will be given in terms of the wave speed

$$C_2 = (M_2/\rho_2)^{1/2} \tag{15}$$

The shear support parameters will be given in terms of

$$k = K/A \tag{16}$$

and

$$f_o = F_o/A \tag{17}$$

The pressure loading function, P(t), chosen for these studies is the triangular pulse, shown in Fig. 4. It is characterized by a peak pressure, P_o, the time of that peak, t_1, and the time at the end of the pulse, t_2 .

In this section certain parameters are fixed as follows

Geometry: H_1 = 20 feet, H_2 = 3.3 feet

Soil: $g\rho_1$ = 110 lb/ft^3, C_L = 1500 ft/sec

Structure: $g\rho_2$ = 150 lb/ft^3, C_2 = 12000 ft/sec

Loading: P_0 = 1 ksi, t_1 = 2 millisec, t_2 = 10 millisec

Finite difference: $N_1 = 40$, $N_2 = 5$

Artificial viscosity: $\alpha_{1/2} = 0$,

$$\alpha_{i+1/2} = 0.04 \quad \text{for } i = 1, 2, \ldots, N_1$$

and $$\alpha_{i+1/2} = 0 \quad \text{for } i = N_1 + 1, \ldots, N_1+N_2+1$$

The remaining parameters are varied as follows

$$U_o = 1, 2, 3, 4$$

$$k = 0, 1, 10 \text{ (kips/in}^3\text{)}$$

Elastic Shear Support ($F_o = \infty$). Stress histories at $x = 20.3$ feet for cases $U_o = 1, 2, 3, 4$ with $k = 0$ (no shear support) are shown in Fig. 5, and the corresponding velocity histories at the interface, $x = 20$ feet, are shown in Fig. 6. Stress histories at $x = 20.3$ feet for $U_o = 1$ with $k = 0, 1, 10$ are shown in Fig. 7, and the corresponding velocities at $x = 20$ feet are shown in Fig. 8. Stress histories at $x = 20.3$ feet for $U_0 = 4$ with $k = 0, 1, 10$ are shown in Fig. 9, and the corresponding velocities at the interface are shown in Fig. 10.

Plastic Shear Support. Results corresponding to plastic behavior of the shear support are presented for various values of f_o so that a ductility of 10 is achieved (iteratively). The ductility is defined as the ratio of maximum displacement of the plastic shear support divided by the displacement at the elastic limit of the support (f_o/k). Stress and velocity histories are shown in Figs. 11 through 14 for the following cases.

Fig. 11: $U_o = 1$, $k = 1$, $f_o = 0.246$

Fig. 12: $U_o = 1$, $k = 10$, $f_o = 0.885$

Fig. 13: $U_o = 4$, $k = 1$, $f_o = 0.122$

Fig. 14: $U_o = 4$, $k = 10$, $f_o = 0.505$

3. UNCOUPLING METHOD - ONE DIMENSIONAL STUDIES

The uncoupling procedure to be studied here is a special case of a more general uncoupling approach described in Appendix A. In the present approximation, the calculation is separated in two parts:

(1) Generation of free-field (no structure) velocities and tractions on the surface located where the external surface of the structure should be.

(2) Structural analysis using the free-field data from (1) in conjunction with the plane wave approximation, where the unload-reloading impedance ($\rho_1 . C_U$) is used for the soil. Let σ_F and v_F denote the free-field stresses and velociites, respectively. The response of the structure is analyzed with the boundary condition

$$\sigma_B = \sigma_F + \rho_1 C_U (v_B - v_F) \tag{18}$$

being used at the surface of the structure, where σ_B and v_B denote the structural boundary stresses and velocities, respectively.

3.1 Free-Field Data, σ_F, v_F

Free-field (no structure) data were calculated by the finite difference method of Eqs. 5, 6, 7 with a soil depth which is sufficiently long (~40 feet) that no reflections from below could affect the solution at x = 20 feet. To reduce errors associated with numerical approximations, the finite difference parameters were made identical to those used in the soil-structure interaction calculations of the preceding section. Hence, $\Delta x_1 = H_1/(N_1 + 1/2)$ with H_1 = 20 feet, N_1 = 40; α = 0.04 for all points. Stresses and velocities at x = 20 feet for U_o = 1 and U_o = 4 are shown in Figs. 15 and 16. Stresses at x = 20 feet were obtained by averaging the two stresses on either side of the particle velocity at this depth.

3.2 Structural Analysis

The response of the structure was analyzed by the finite difference method of Eqs. 7, 8, 9, 11, 12, with the soil mass ignored in Eq. 12; the structural boundary stress in Eq. 12 was based on Eq. 18

$$\sigma_i^n = \sigma_F^n + \rho_1 C_U (v_i^n - v_F^n) \quad \text{for } i = N_1 + 1 \qquad (19)$$

The accuracy of this uncoupling approximation can be evaluated by studying the calculated velocity time history at the boundary, since the response of the structure is completely determined by this quantity.

Figure 17 shows the velocity time history for the case, $U_o = 1$, $k = 0$, (no shear support) with the corresponding soil-structure interaction results from Fig. 8. This is simply the plane wave approximation for the elastic case and, as expected, the comparison is excellent. Similarly, the comparisons in Fig. 18 for $U_o = 1$, $k = 1$, $f_o = \infty$, and in Fig. 19 for $U_o = 1$, $k = 10$, $f_o = \infty$, are both excellent.

Figure 20 shows the comparison for $U_o = 4$, $k = 0$, $f_o = \infty$ with the corresponding soil-structure interaction results from Fig. 10. Similarly the comparison for $U_o = 4$, $k = 1$, $f_o = \infty$ is shown in Fig. 21; the comparison for $U_o = 4$, $k = 10$, $f_o = \infty$ is shown in Fig. 22. In these cases, the soil is hysteretic but the structure is elastic.

Figure 23 shows the comparison for $U_o = 1$, $k = 1$, $f_o = 0.246$ with the results from Fig. 12. The comparison for $U_o = 1$, $k = 10$, $f_o = 0.885$ is shown in Fig. 24. In these cases the structure responds plastically but the soil is elastic.

Figure 25 shows the comparison for $U_o = 4$, $k = 1$, $f_o = 0.122$ with the results from Fig. 14. The comparison for $U_o = 4$, $k = 10$, $f_o = 0.505$ is shown in Fig. 26. In these cases the soil is hysteretic and the structure behaves plastically.

3.3 Single-Degree-of-Freedom Results

The finite difference calculations in Section 2 and in this section so far were done with five stress points in the structure ($N_2 = 5$). However, it is interesting to note that waves propagate relatively fast in the structure so that the velocity time histories in Figs. 17 through 26 can be reproduced quite well by representing the structure as a single-degree-of-freedom particle with velocity v and mass per unit area $m = \rho_2 H_2$. The equation of motion, including the uncoupling approximation, then becomes

$$m\dot{v} = -[\sigma_F + \rho_1 C_U (v_F - v)\ ] + \frac{F_S}{A} \tag{20}$$

Figures 27 through 30 show selected comparisons of velocity time histories obtained using Eq. 20, with corresponding case results for $N_2 = 5$. The differences are quite small even in the nonlinear problems.

3.4 Variation of Soil Impedance

All results so far have been based on a constant value of $\rho_1 C_U$ for the soil impedance in the uncoupling approximation. This choice can be seen to be a good one for the present studies by examining Fig. 31 where the results of using the loading impedance $\rho_1 C_L$ are compared with the corresponding case results using $\rho_1 C_U$ and the interaction results from Section 2. The very early time results using $\rho_1 C_L$ compare better with the interaction results but once unloading begins, the difference becomes noticeable. Still, it is interesting to note that even though the soil impedance was changed by a factor of two, the later-time error is only about thirty per cent. Thus, the choice of the soil impedance seems to be less critical than one might expect.

Other ways of choosing the soil impedance in the uncoupling approximation may be considered. For example, it might seem that the impedance could be made to depend upon the state of t! soil by first choosing $\rho_1 C_L$ when σ_F initially loads the structure, then switching to $\rho_1 C_U$ once σ_F indicates unload-reloading behavior is taking place in the soil. This has been tried and the results are not substantially altered by this procedure except for the introduction of some high-frequency numerical oscillations. These oscillations are the result of a change in acceleration whose magnitude depends on $\rho_1(C_U - C_L)$, the current magnitude of v, and the time increment Δt. Such numerically activated accelerations are quite undesirable and should be avoided. Smooth variations of the impedance may be used but since the initial loading phase is so brief for explosive loadings, the use of $\rho_1 C_U$ at all times seems to be a reasonable approximation, at least until further study is made. If the soil's unload-reloading behavior is known, then a smoothly varying impedance may be considered. (However, in many situations, $\rho_1 C_U$ is only known roughly and a constant value may be acceptable.) Additional study may be needed in this area, see Ref. [5].

4. MULTI-DIMENSIONAL CONSIDERATIONS

The multi-dimensional generalization of the uncoupling approximation, Eq. 18 (see also Appendix A, Eq, A-6), can be written as

$$\underset{\sim}{t}_B = \underset{\sim}{t}_F + \rho \underset{\approx}{c} \cdot (\underset{\sim}{v}_B - \underset{\sim}{v}_F) \tag{21}$$

where $\underset{\sim}{t}_F$ and $\underset{\sim}{v}_F$ are free-field traction and velocity vectors at the surface where the structure should be, and $\underset{\sim}{t}_B$ and $\underset{\sim}{v}_B$ are traction and velocity vectors at the boundary of the structure. From wave propagation considerations, the form of the tensor $\underset{\approx}{c}$ can be expressed as

$$\underset{\approx}{c} = \pm \begin{bmatrix} c_p & 0 & 0 \\ 0 & c_s & 0 \\ 0 & 0 & c_s \end{bmatrix} \tag{22}$$

where $\underset{\approx}{c}$ is given in a local coordinate system whose first coordinate corresponds to the outward normal of the surface of the structure, and the sign is chosen to produce outward wave propagation (radiation damping); c_p and c_s are the speeds of dilatational and shear waves, respectively, in the soil. As mentioned in the previous section, a smooth variation in the unload-reloading behavior can be introduced into $\underset{\approx}{c}$, if necessary.

The geometry of a particular situation can affect the way in which the uncoupling approximation is used. In Fig. 1, for example, waves will be reflected back and forth between the roof and the ground surface. This effect would have been noticeable in the results of the previous section if the calculations had been carried out much further in time. This effect, while noticeable in the one-dimensional case, is not likely to be important in two- and three-dimensional problems where the depth of the roof is on the order of one or more times the horizontal span of the structure. The

importance of such geometrical effects must be considered carefully in a particular analysis since the free-field data do not include these effects.

A refinement of the uncoupling approximation can be used to include geometrical effects, if necessary. First, instead of a free-field calculation, a soil-structure interaction calculation is made with a coarse model of the structure, and tractions and velocities are recorded at points on the exterior of the structure. These tractions and velocities are then used in place of the free-field data in Eq. 21 with a suitably refined model of the structure. It is also possible to record tractions and velocities on the surface of an imaginary convex surface outside the structure and then use a refined model of the soil and structure inside this surface. The major drawback to using this approach is that the first stage calculation will generally be more complicated and hence more costly than a free-field calculation. Detailed studies involving multi-dimensional situations are in progress and will be reported separately.

5. SUMMARY AND CONCLUSIONS

An uncoupling approximation for analyzing explosively loaded structures embedded in hysteretic media has been presented. The method, based on wave propagation considerations, can be viewed as the plane wave approximation extended to nonlinear media. Its accuracy has been shown to be quite good for a series of one-dimensional soil-sturcture interaction problems, even when the structure and surrounding soil are both nonlinear.

It should be noted that both free-field traction and velocity vectors must be known or calculated in order to apply the method. In addition, the soil's unload-reloading behavior is required.

Multi-dimensional problems, and techniques for improving the method, were also described briefly. Further development and experience are needed, but it appears that reasonably accurate results can be obtained by judicious application of these techniques.

REFERENCES

[1] "H.H. Bleich, "Dynamic Interaction Between Structures and Fluid", in Structural Mechanics, Pergamon Press, pp. 263-284, 1960.

[2] F.L. DiMaggio, I.S. Sandler and D. Rubin, "Uncoupling Approximation in Fluid-Structure Interaction Problems with Cavitation", DNA Report 5191T, Weidlinger Associates, New York, January 1980.

[3] F.S. Wong, "A Study of the Effect of Structure-Medium Interaction on the Loading on a Buried Structure", Report No. 7864, Weidlinger Associates, Menlo Park, California (for U.S. Army Corps of Engineers, MEDED-MM), November 1978.

[4] F.S. Wong, "Transfer Function Development for Shallow-Buried Rectangular Boxes", Report No. 8034, Weidlinger Associates, Menlo Park, California, (for Air Force Weapons Laboratory), June 1980.

APPENDIX

INTERACTIVE SCHEMES FOR NONLINEAR MEDIA

Consider a structure S partially or totally embedded in a nonlinear medium M. Let B be the surface common to S and M. Assume that free field input is available and could be used in a simplified structure-medium calculation in which only a coarse approximation of the structure is used. This solution gives trial boundary tractions $\underset{\sim}{t}_B^T$.

Let the correct boundary tractions for the actual structure be denoted by $\underset{\sim}{t}_B$. Due to the error $\underset{\sim}{t}_B^T - \underset{\sim}{t}_B$ in the tractions in the simplified calculation, the velocities along B are in error by an amount $v_B^T - v_B$ as determined by

$$\underset{\sim}{t}_B^T - \underset{\sim}{t}_B = \underset{\approx}{F}\{\underset{\sim}{v}_B^T - \underset{\sim}{v}_B\} \tag{A-1}$$

where $\underset{\approx}{F}$ is a functional which describes the response of the surrounding material to an excitation on boundary B. The proposed uncoupling procedure consists of finding an appropriate approximation to functional $\underset{\approx}{F}$.

For a general nonlinear structure, finite element equations will be of the form

$$\phi(\underset{\sim}{x}) = \underset{\sim}{P} \tag{A-2}$$

in which $\underset{\sim}{x}$ and $\underset{\sim}{P}$ are the displacement and interface force vectors, respectively, and ϕ is an operator which represents the structural characteristics. If $\underset{\sim}{t}_B^T$ and $\underset{\sim}{t}_B$ are first Piola-Kirchhoff tractions, $\underset{\sim}{P}$ depends linearly on the interface tractions $\underset{\sim}{t}_B$, i.e.,

$$\underset{\sim}{P} = \underset{\sim}{P}(\underset{\sim}{t}_B^T) - \underset{\sim}{P}(\underset{\sim}{t}_B^T - \underset{\sim}{t}_B) \tag{A-3}$$

Then (A-2) may be written as

$$\phi(\underset{\sim}{x}) + \underset{\sim}{P}[\underset{\approx}{F}(\underset{\sim}{v}_B^T - \underset{\sim}{v}_B)] = \underset{\sim}{P}(\underset{\sim}{t}_B^T) \tag{A-4}$$

The left hand side of (A-4) represents a modified structural operator in which the boundaries of the actual structure are supported by nonlinear hysteretic connections to a base which moves with velocity $\underset{\sim}{v}_B^T$. The right hand side represents the interface loading from the trial calculation.

In physical terms this means that the traction $\underset{\sim}{t}_B^T$ can be used to load the actual structure. However, to account for the fact that $\underset{\sim}{t}_B^T$ corresponds to a slightly different structure, the boundary supports of the actual structure are modified by the use of non-linear supports. These supports are attached to a base with the approximate motion $\underset{\sim}{v}_B^T$ to the structure at each of its nodes or velocity points. The support behavior $\underset{\approx}{F}$ is chosen so as to represent the appropriate loading/unloading/reloading behavior of the medium surrounding the structure.

As a first choice, take

$$\underset{\approx}{F} = \rho \underset{\approx}{c} \tag{A-5}$$

so that (A-1) becomes

$$\underset{\sim}{t}_B^T - \underset{\sim}{t}_B = \rho \underset{\approx}{c} \cdot (\underset{\sim}{v}_B^T - \underset{\sim}{v}_B) \tag{A-6}$$

in which $\underset{\approx}{c}$ is a tensor formea from the wave speeds in the medium. This is equivalent to the plane wave approximation used for linear media and involves only linear dashpot supports on the structure. Similarly, $\underset{\approx}{F}$ can be chosen to give an interactive scheme analogous to the doubly asymptotic approximation.

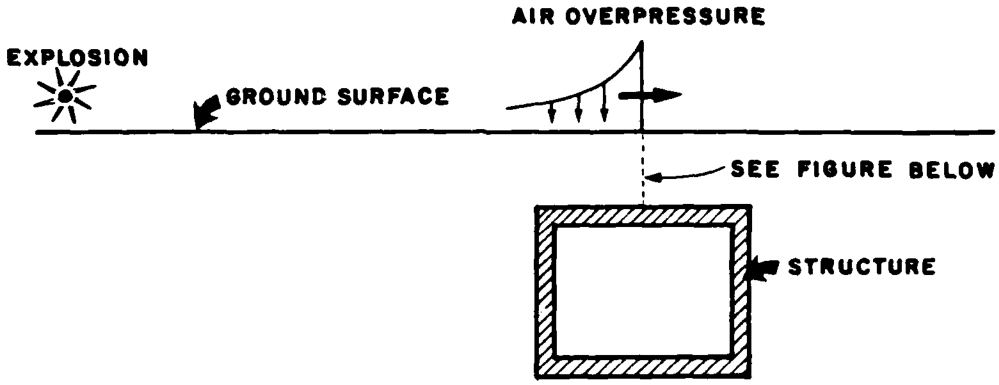

FIG I. A SOIL - STRUCTURE INTERACTION PROBLEM

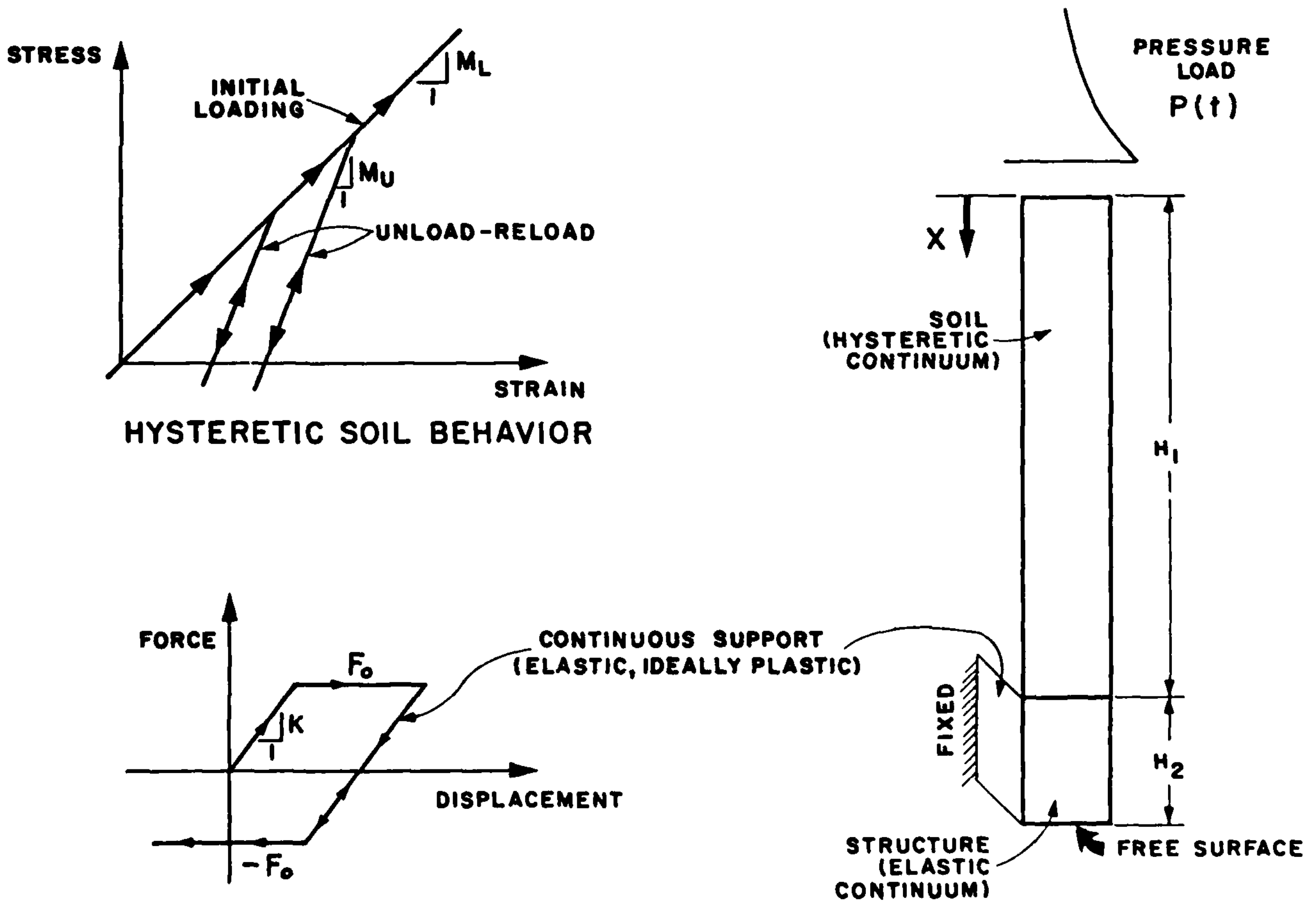

FIG 2. ONE DIMENSIONAL SOIL-STRUCTURE INTERACTION MODEL

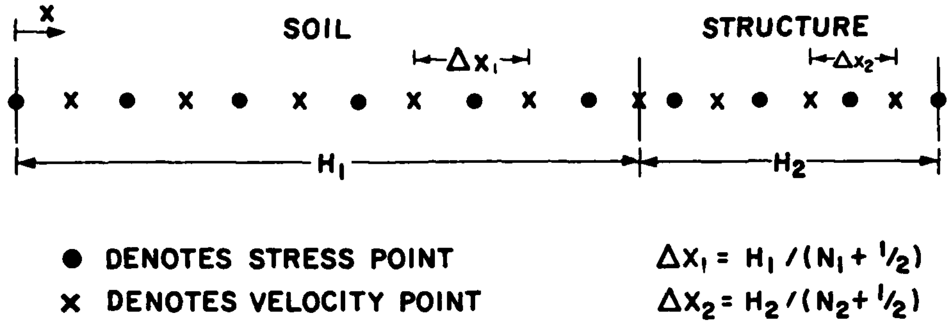

FIG. 3 STAGGERED FINITE DIFFERENCE GRID FOR ONE DIMENSIONAL STUDIES.

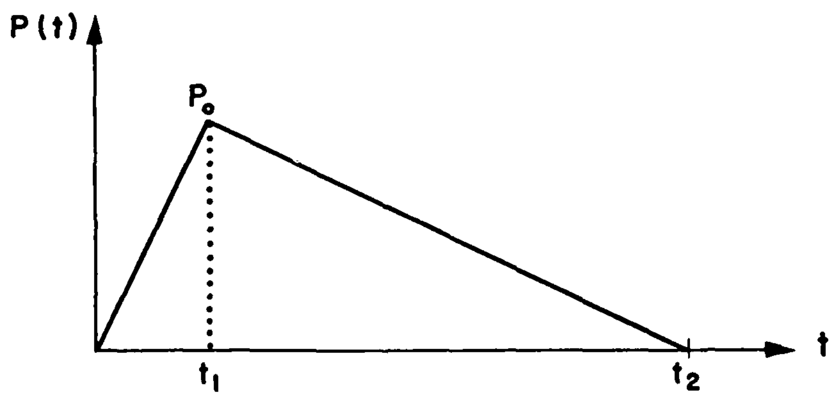

FIG 4 PRESSURE LOADING USED IN ONE DIMENSIONAL STUDIES

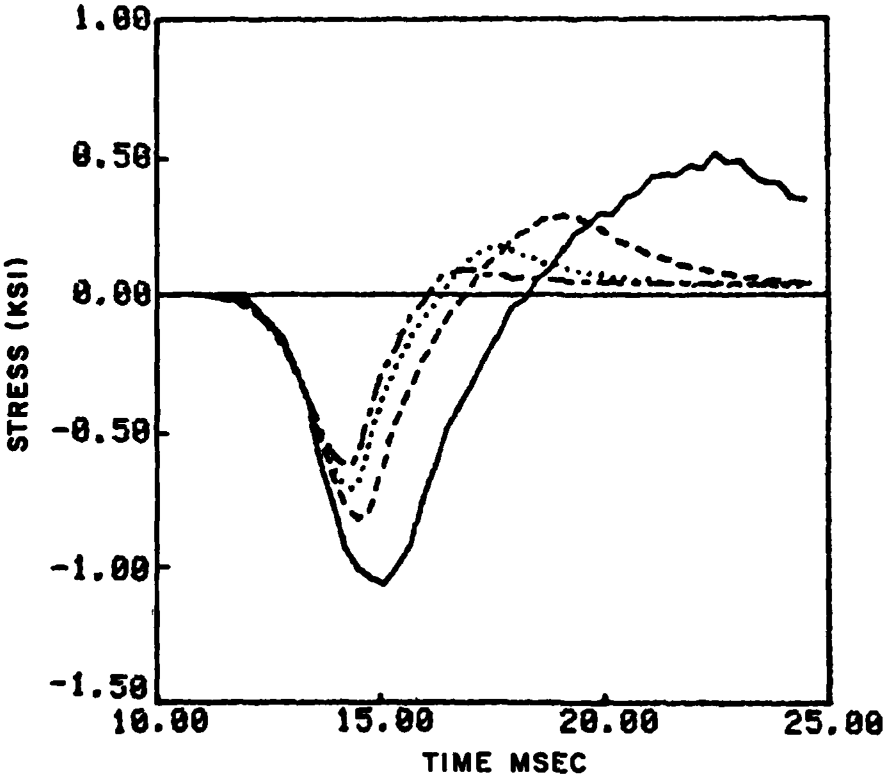

FIG. 5 STRESS HISTORIES AT 20.3 FEET FOR SOIL UNLOADING CASES $U_o = 1,2,3,4$ WITH $k=0$, $f_o = \infty$ (NO SHEAR SUPPORT)

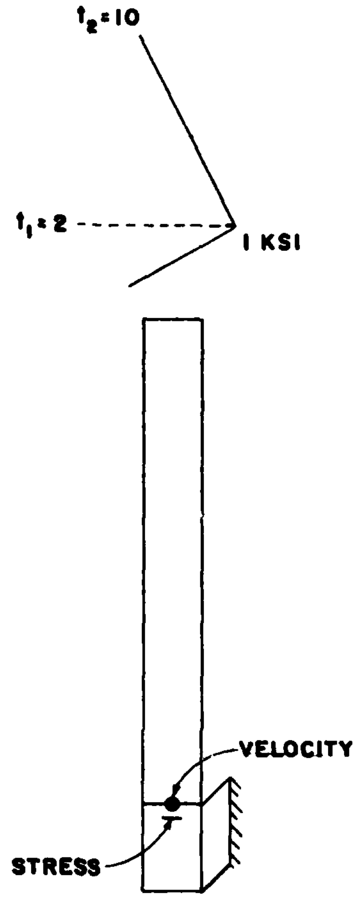

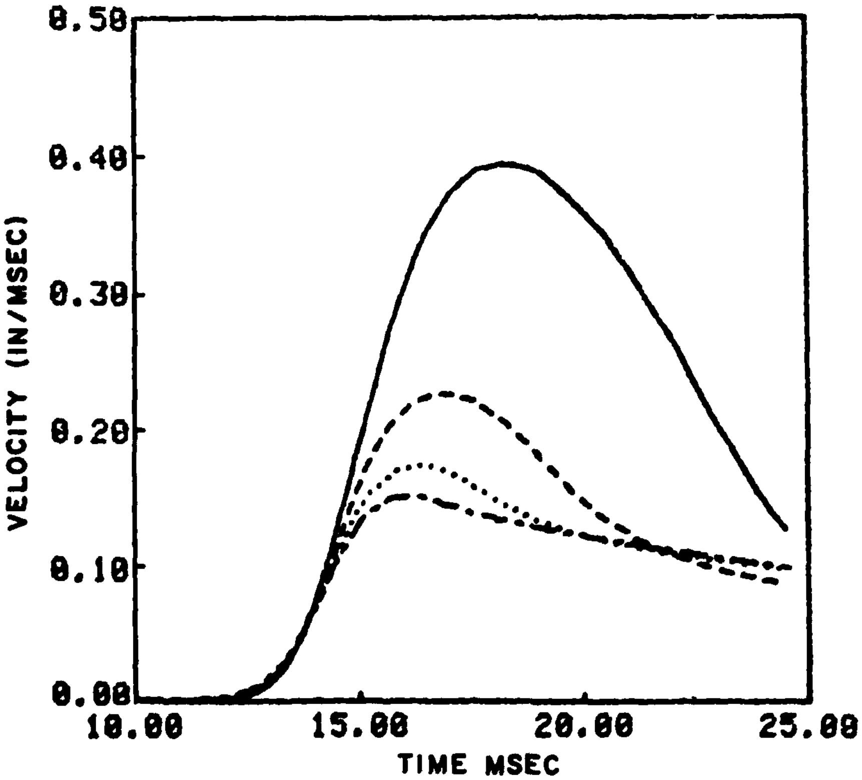

FIG. 6 VELOCITY HISTORIES AT 20 FEET FOR SOIL UNLOADING CASES $U_o = 1,2,3,4$ WITH $k = 0$, $f_o = \infty$ (NO SHEAR SUPPORT)

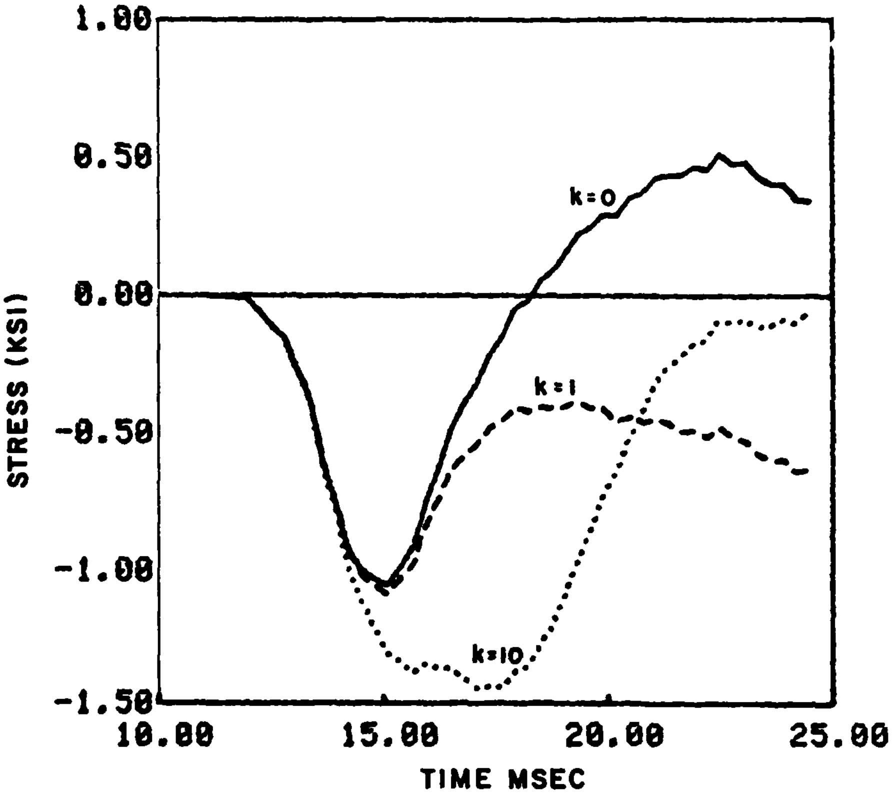

FIG. 7 STRESS HISTORIES AT 20.3 FEET FOR ELASTIC SOIL (U_o= 1) AND ELASTIC SHEAR SUPPORTS (k = 0,1,10)

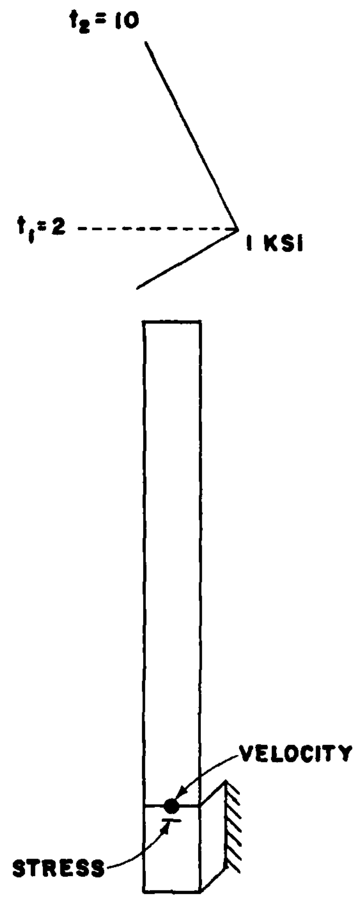

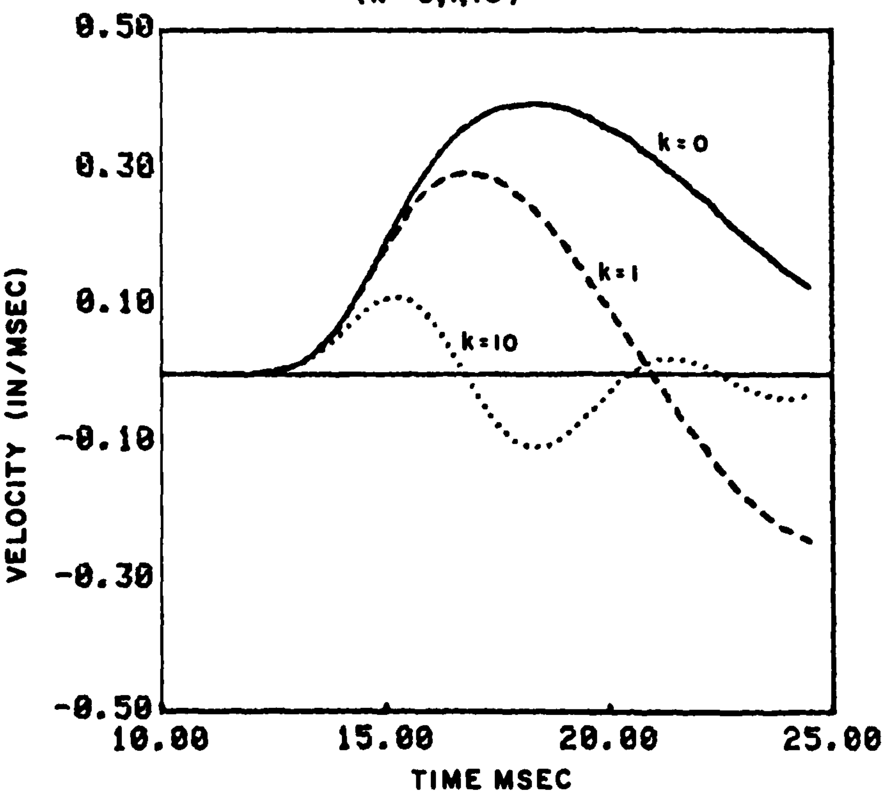

FIG. 8 VELOCITY HISTORIES AT 20 FEET FOR ELASTIC SOIL (U_o=1) ELASTIC SHEAR SUPPORTS (k=0,1,10)

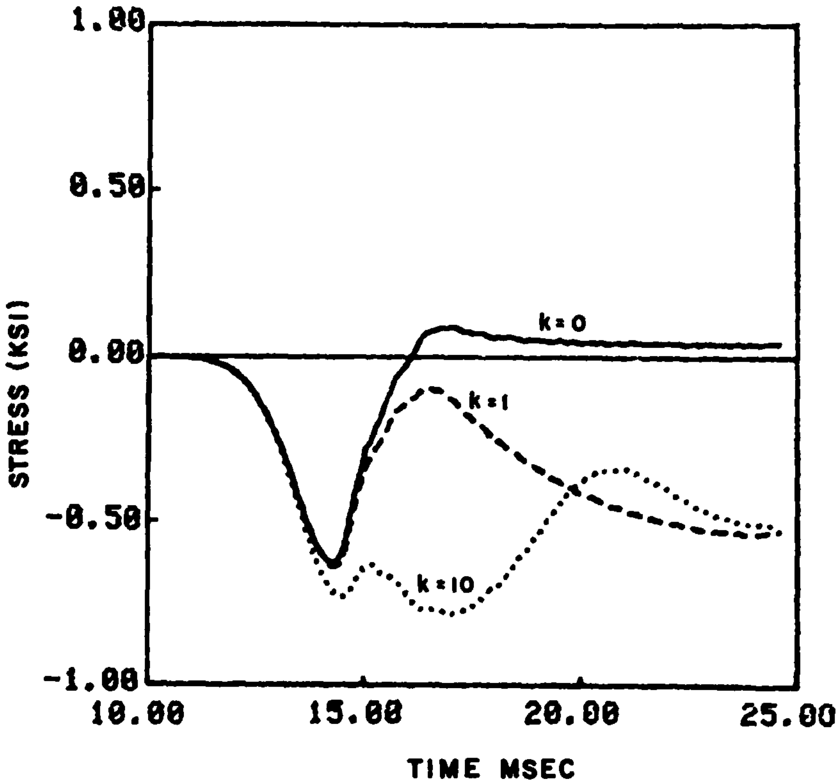

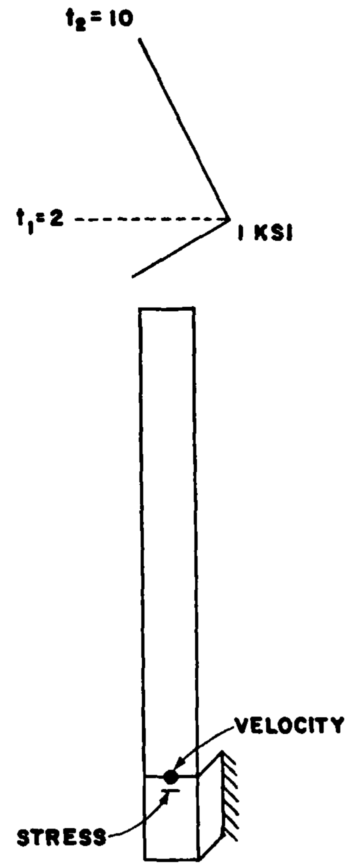

FIG. 9 STRESS HISTORIES AT 20.3 FEET FOR HYSTERETIC SOIL (U_o=4) AND ELASTIC SHEAR SUPPORTS (k=0,1,10)

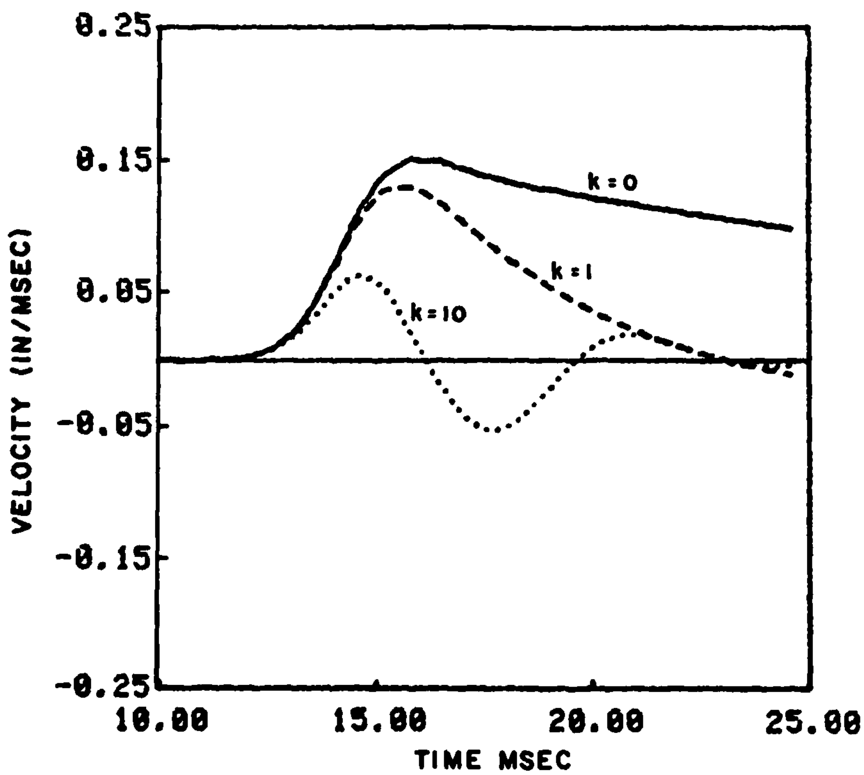

FIG. 10 VELOCITY HISTORIES AT 20 FEET FOR HYSTERETIC SOIL (U_o=4) AND ELASTIC SHEAR SUPPORTS (k = 0, 1, 10)

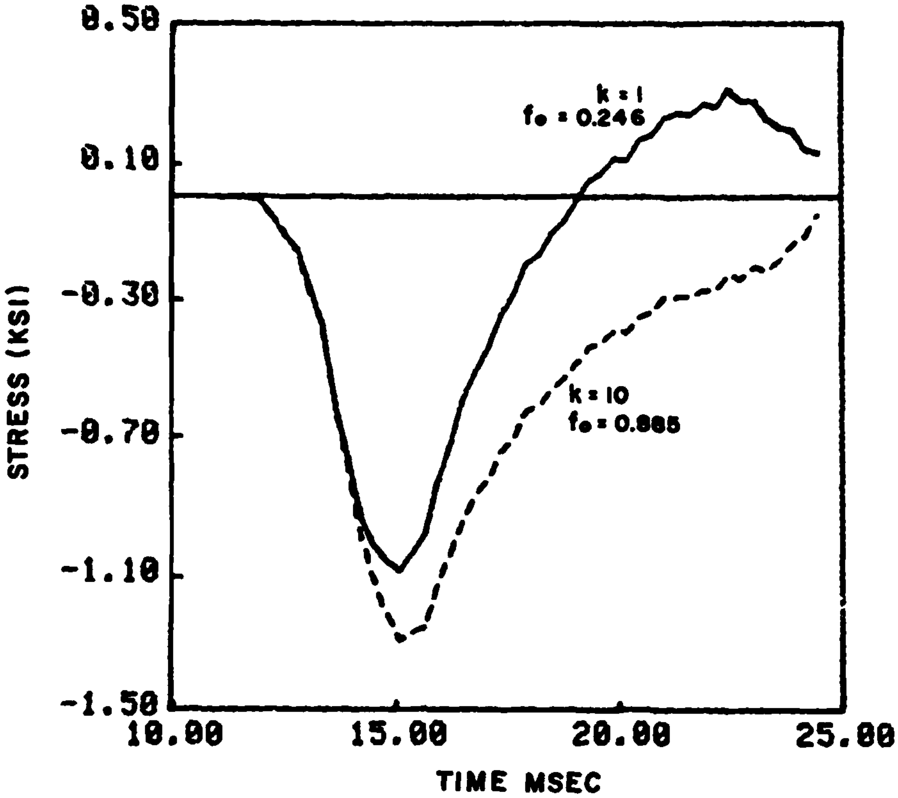

FIG. 11 STRESS HISTORIES AT 20.3 FEET FOR ELASTIC SOIL ($U_o = 1$) AND PLASTIC SHEAR SUPPORTS.

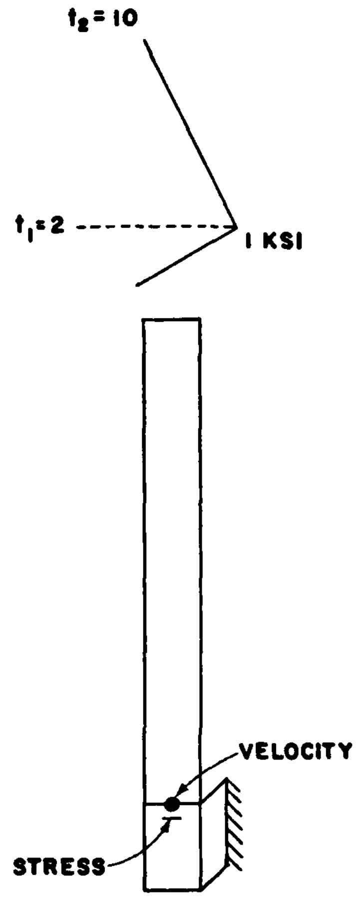

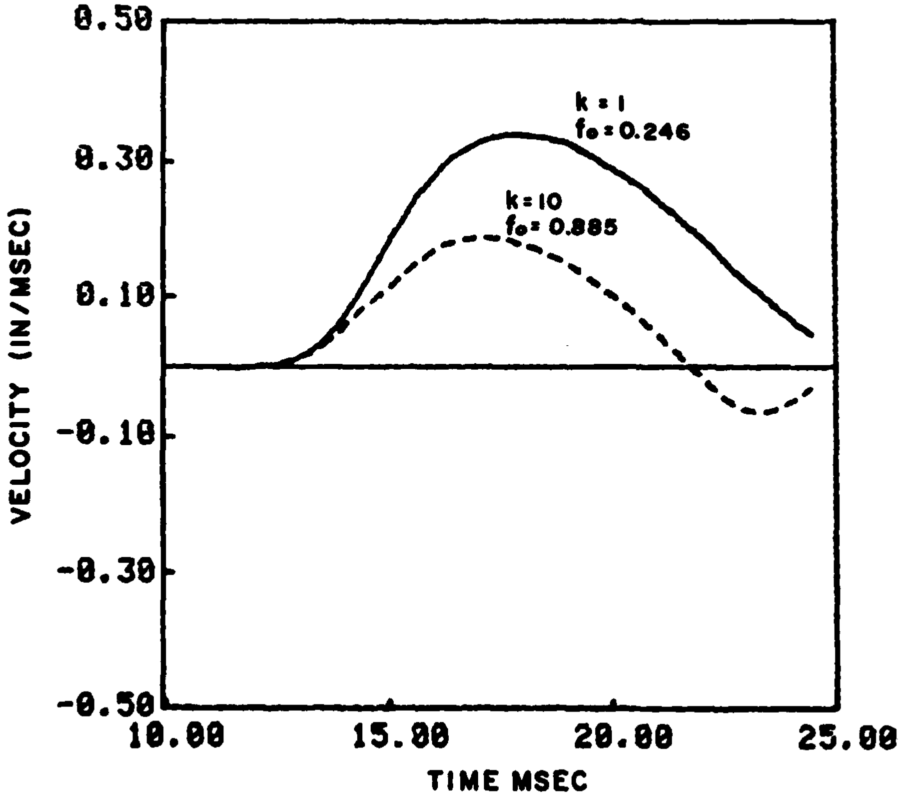

FIG. 12 STRESS HISTORIES AT 20 FEET FOR ELASTIC SOIL ($U_o = 1$) AND PLASTIC SHEAR SUPPORTS

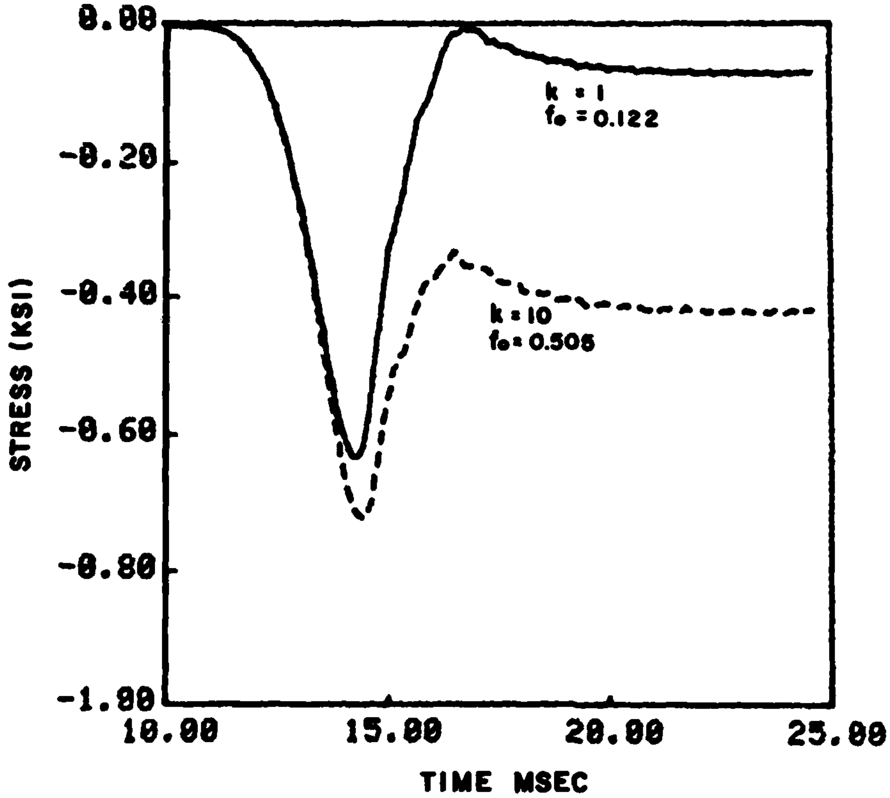

FIG. 13 STRESS HISTORIES AT 20.3 FEET FOR HYSTERETIC SOIL (U_o = 4) AND PLASTIC SHEAR SUPPORTS

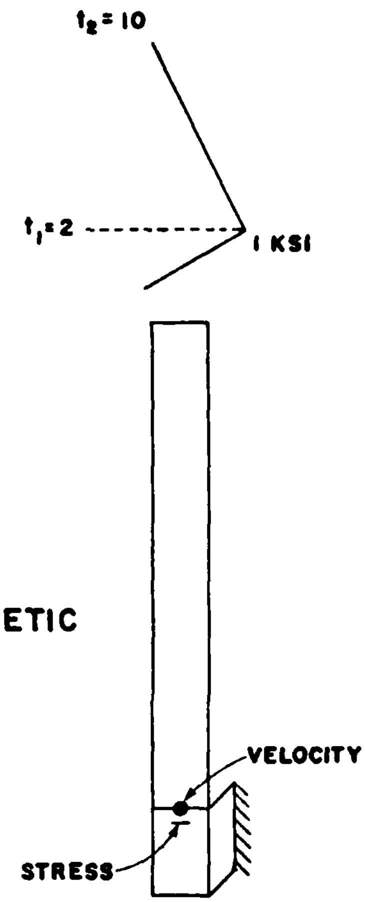

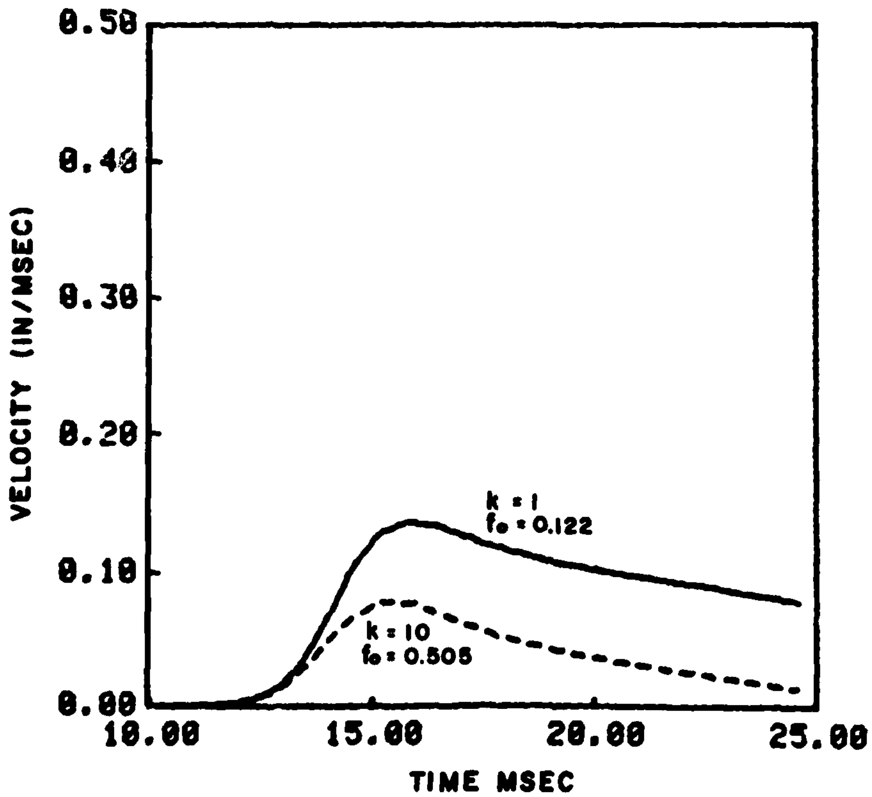

FIG. 14 VELOCITY HISTORIES AT 20 FEET FOR HYSTERETIC SOIL (U_o = 4) AND PLASTIC SHEAR SUPPORTS

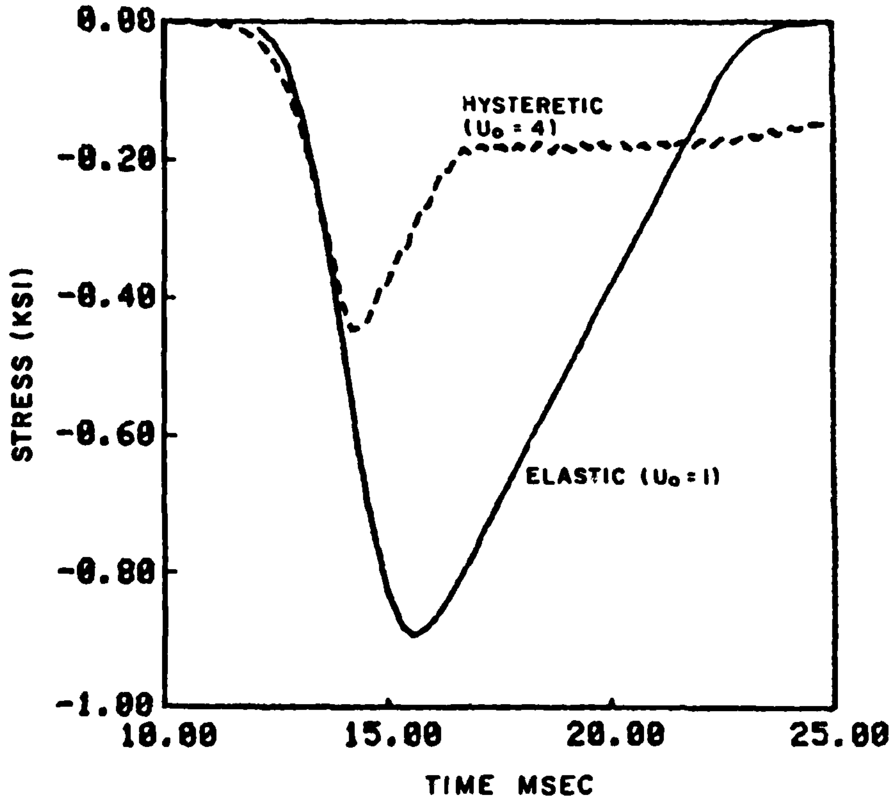

FIG. 15 FREE-FIELD STRESSES (AVERAGED) AT 20 FEET FOR ELASTIC (U_o = 1) AND HYSTERETIC (U_o = 1) SOILS

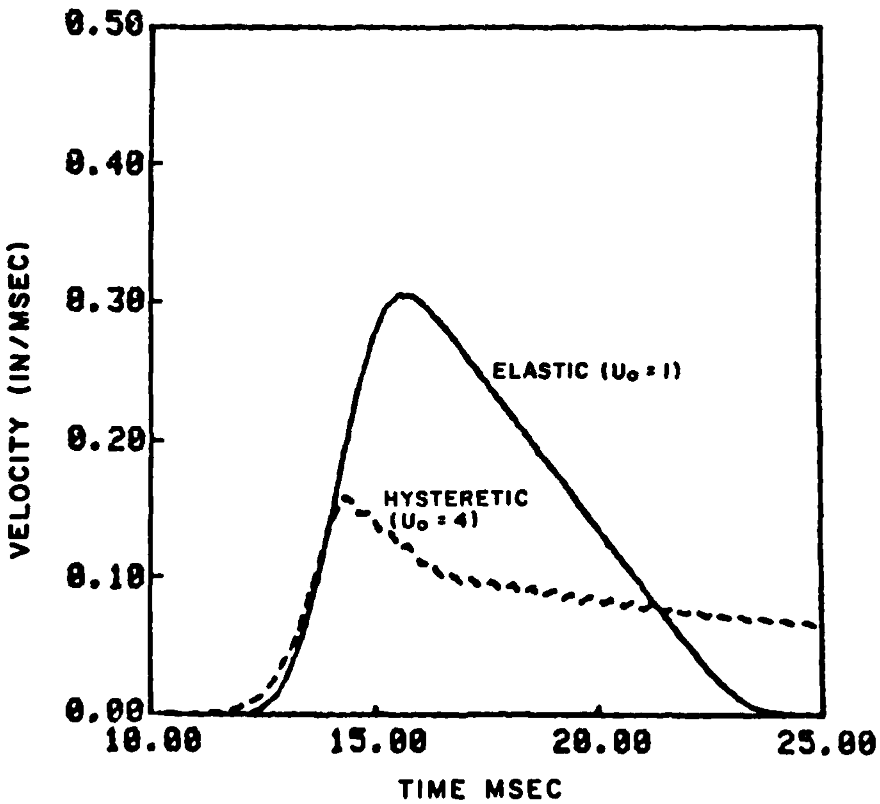

FIG. 16 FREE FIELD VELOCITIES AT 20 FEET FOR ELASTIC (U_o = 1) AND HYSTERETIC (U_o = 4) SOILS.

COMPARISON OF RESULTS FROM UNCOUPLING APPROXIMATION WITH SOIL-STRUCTURE INTERACTION

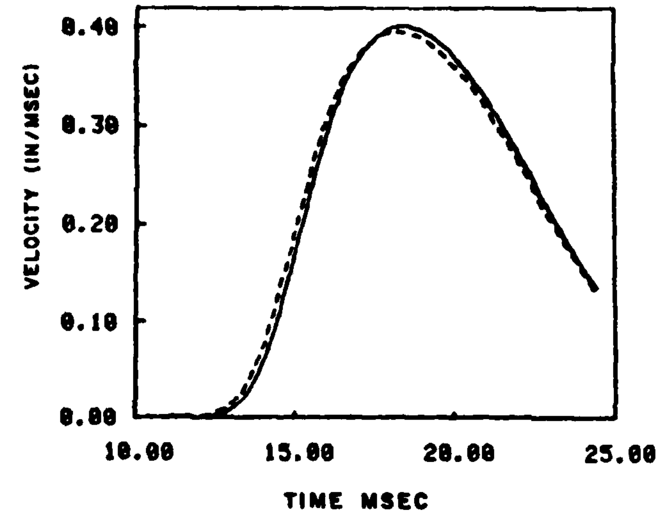

FIG. 17

ELASTIC ($U_o = 1$) SOIL,
NO SHEAR SUPPORT (k = 0)

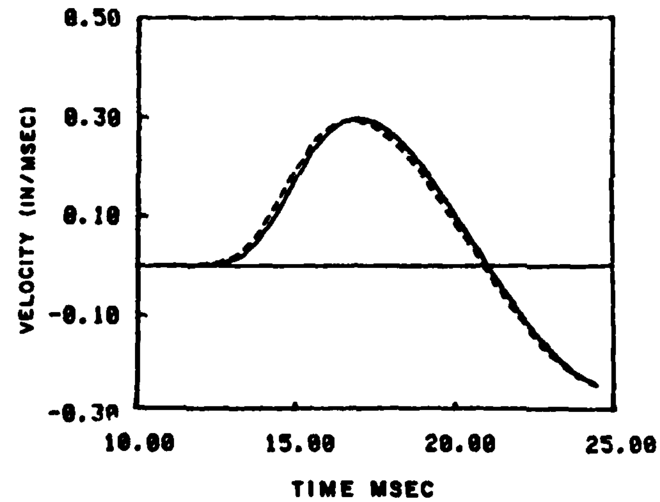

FIG. 18

ELASTIC ($U_o = 1$) SOIL,
ELASTIC (k=1) SHEAR SUPPORT

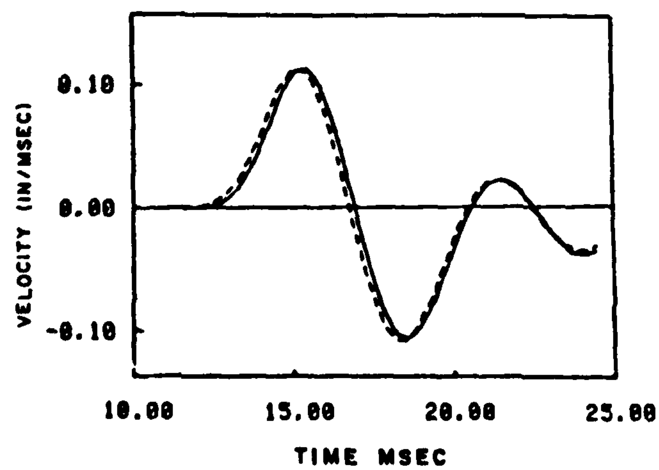

FIG. 19

ELASTIC ($U_o = 1$) SOIL,
ELASTIC (k=10) SHEAR SUPPORT

COMPARISON OF RESULTS FROM UNCOUPLING APPROXIMATION WITH SOIL-STRUCTURE INTERACTION

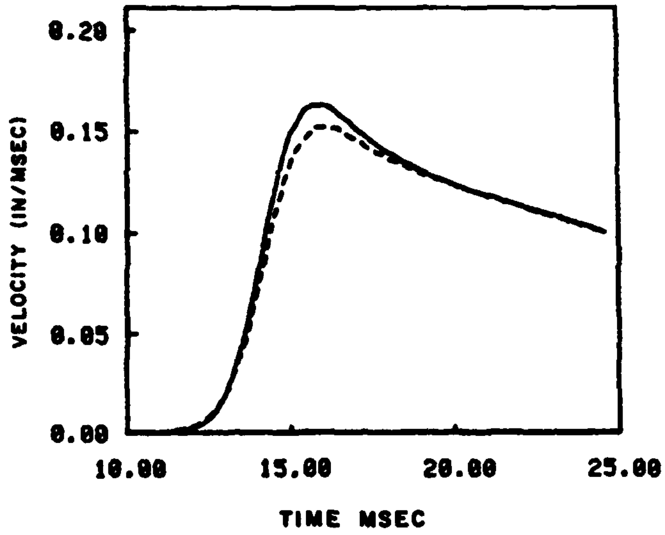

FIG. 20
HYSTERETIC ($U_o = 4$) SOIL, NO SHEAR SUPPORT ($k=0$)

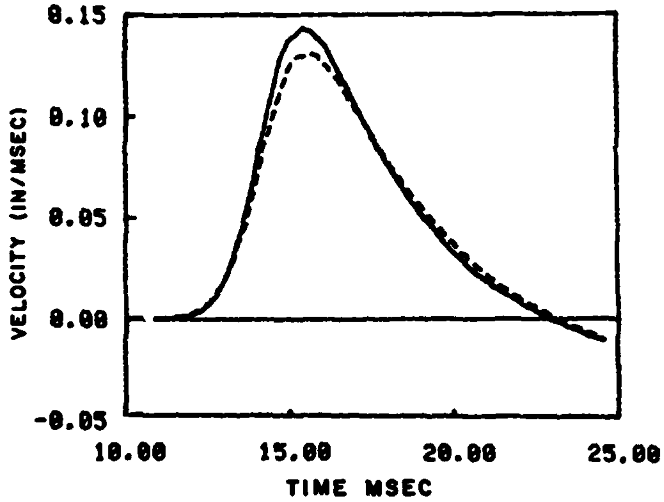

FIG. 21
HYSTERETIC ($U_o = 4$) SOIL, ELASTIC ($k=1$) SHEAR SUPPORT

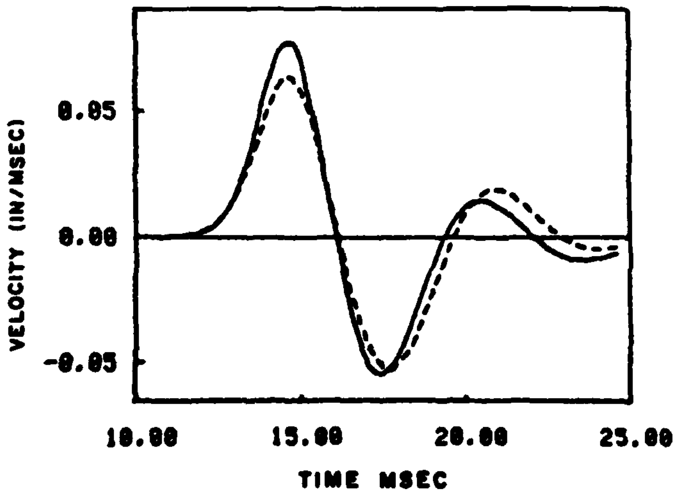

FIG. 22
HYSTERETIC ($U_o = 4$) SOIL, ELASTIC ($k=10$) SHEAR SUPPORT

COMPARISON OF RESULTS FROM UNCOUPLING APPROXIMATION WITH SOIL-STRUCTURE INTERACTION

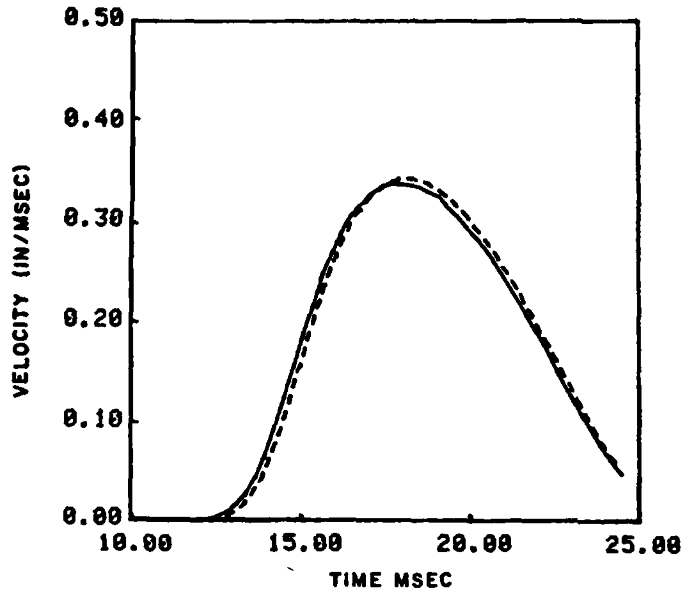

FIG. 23
ELASTIC (U_o=1) SOIL,
PLASTIC (k=1, f_o=0.246)
SHEAR SUPPORT

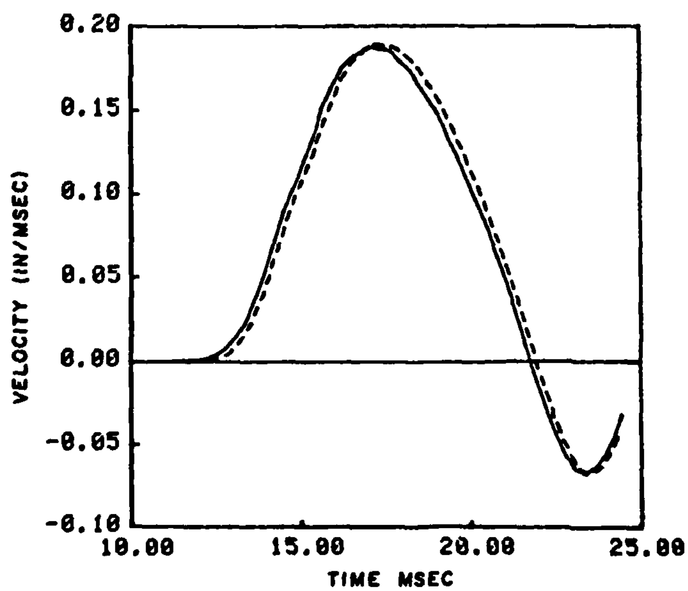

FIG. 24
ELASTIC (U_o=1) SOIL,
PLASTIC (k=10, f_o=0.885)
SHEAR SUPPORT

COMPARISON OF RESULTS FROM UNCOUPLING APPROXIMATION WITH SOIL-STRUCTURE INTERACTION

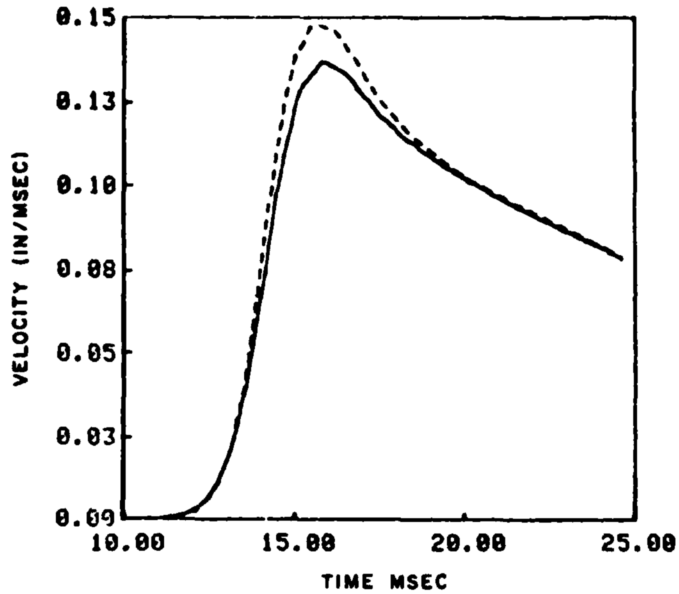

FIG. 25
HYSTERETIC (U_o=4) SOIL,
PLASTIC (k=1, f_o= 0.122)
SHEAR SUPPORT

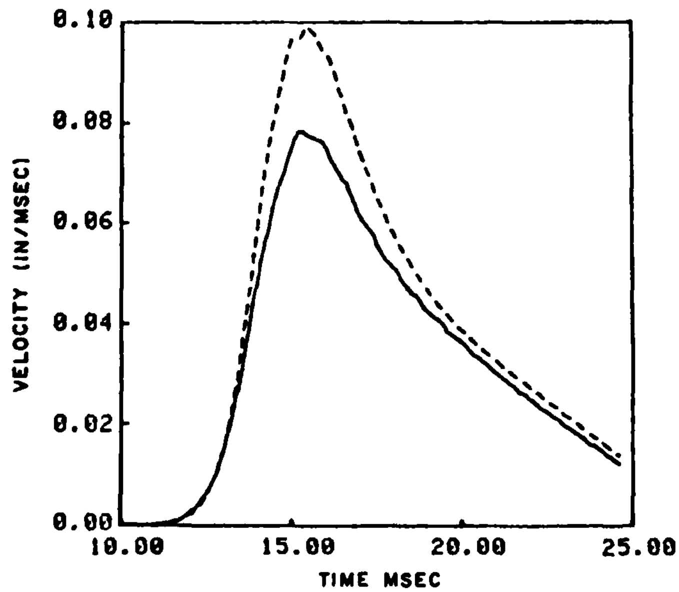

FIG. 26
HYSTERETIC (U_o=4) SOIL,
PLASTIC (k=10, f_o = 0.505)
SHEAR SUPPORT

COMPARISON OF S D O F STRUCTURAL MODEL WITH UNCOUPLING APPROXIMATION AND SSI MODEL

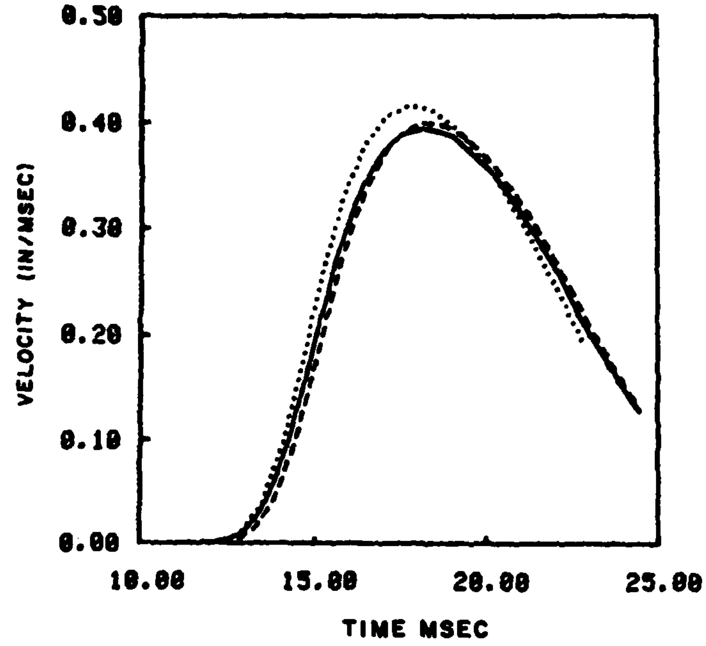

FIG. 27
ELASTIC (U_o = 1) SOIL, NO (k = 0) SHEAR SUPORT

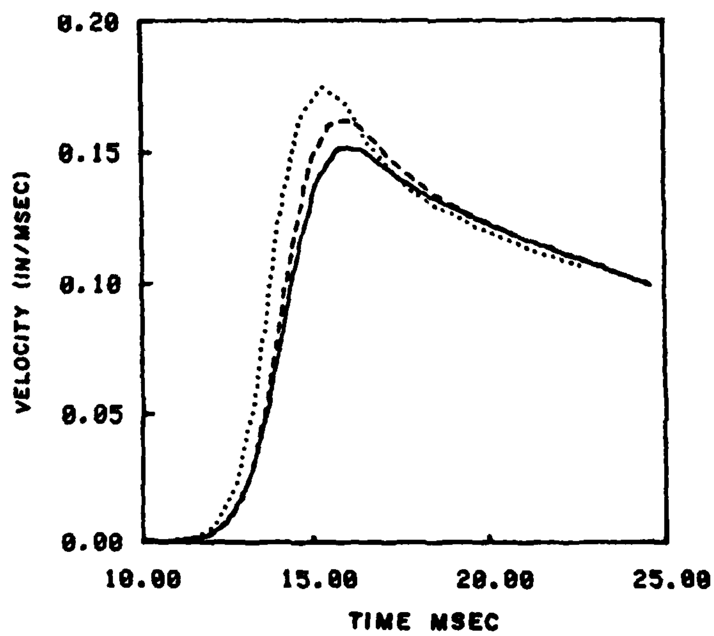

FIG. 28
HYSTERETIC (U_o = 4) SOIL, NO (k = 0) SHEAR SUPPORT

COMPARISON OF S D O F STRUCTURAL MODEL WITH UNCOUPLING APPROXIMATION AND SSI MODEL

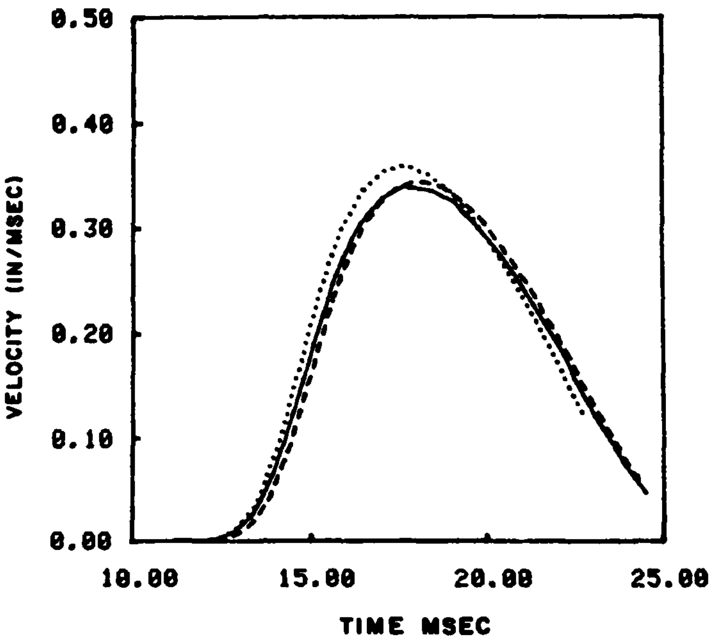

FIG. 29
ELASTIC (U_o = 1) SOIL,
PLASTIC (k = 1, f_o = 0.246)
SHEAR SUPPORT

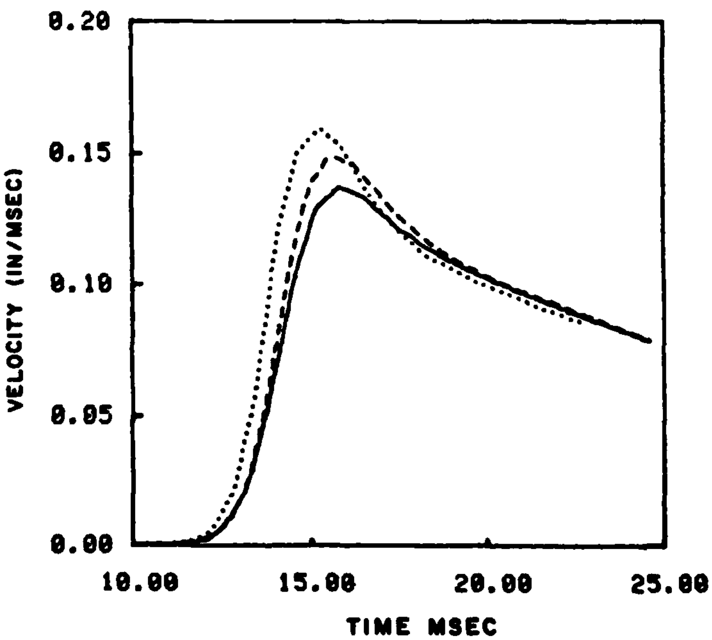

FIG. 30
HYSTERETIC (U_o = 4) SOIL,
PLASTIC (k = 1, f_o = 0.122)
SHEAR SUPPORT

COMPARISON OF UNCOUPLING APPROXIMATION
BASED ON TWO DIFFERENT SOIL IMPEDANCES WITH SSI MODEL

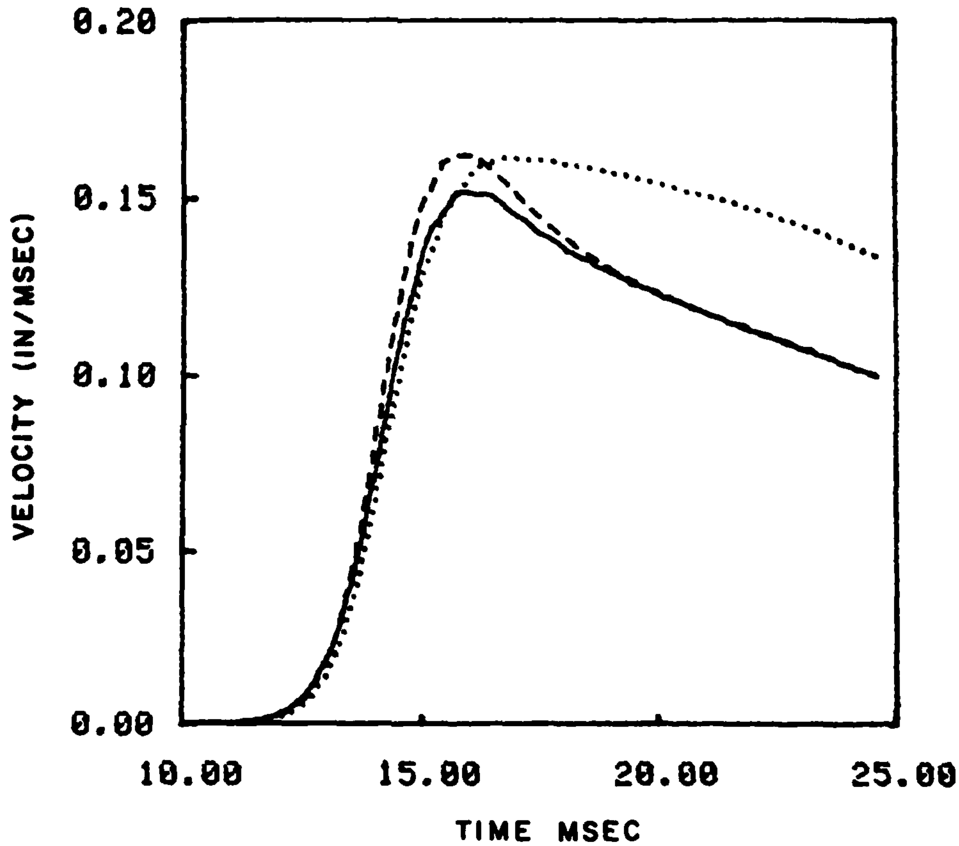

FIG. 31 HYSTERETIC ($U_o=4$) SOIL, NO ($k=0$) SHEAR SUPPORT

DISTRIBUTION LIST

DEPARTMENT OF DEFENSE

Defense Intell Agency
ATTN: DB-4C2, C. Wiehle
ATTN: S. Halperson
ATTN: RDS-3A

Defense Nuclear Agency
ATTN: STSP
2 cy ATTN: SPSS
4 cy ATTN: TITL

Defense Tech Info Ctr
12 cy ATTN: DD

Field Command
Defense Nuclear Agency
ATTN: FCTMOF

Interservice Nuc Weapons School
ATTN: TTV

Joint Strat Tgt Planning Staff
ATTN: JLTW-2

Under Secy of Def for Rsch & Engrg
ATTN: Strat & Space Sys, OS

DEPARTMENT OF THE ARMY

BMD Advanced Technology Ctr
ATTN: 1 CRDABH-X
ATTN: ATC-T

Chief of Engineers
ATTN: DAEN-MCE-D
ATTN: DAEN-RDL

Construction Engrg Rsch Lab
ATTN: W. Fisher

Dep Ch of Staff for Rsch Dev & Acq
ATTN: DAMA-CSS-N, Spt Sys Div, Nuc TM

Engrg Studies Ctr
ATTN: DAEN-FES

Harry Diamond Labs
ATTN: DELHD-TA-L
ATTN: DELHD-NW-P

US Army Ballistic Research Labs
ATTN: DRDAR-BLT, J. Keefer
ATTN: DRDAR-BLV

US Army Comm Cmd
ATTN: Tech Reference Div

US Army Engrg Ctr & Ft Belvoir
ATTN: ATZA-CDC
ATTN: ATZA-DTE-ADM

US Army Engrg Div Huntsville
ATTN: HNDED-SR

US Army Engrg Div Ohio River
ATTN: ORDAS-L

DEPARTMENT OF THE ARMY (Continued)

US Army Engrg Waterways Exper Station
ATTN: WESSA, W. Flathau
ATTN: WESSD, J. Jackson
ATTN: Library
ATTN: J. Strange
ATTN: J. Zelasko
ATTN: WESSE
ATTN: WESSS, J. Ballard
ATTN: F. Brown

US Army Mobility Equip R&D Cmd
ATTN: DRDME-WC
ATTN: DRDME-HT, A. Tolbert

US Army Nuc & Chem Agency
ATTN: Library

US Army War College
ATTN: Library

USA Military Academy
ATTN: Document Library

USA Missile Command
ATTN: RSIC
ATTN: DRSMI-XS

DEPARTMENT OF THE NAVY

David Taylor Naval Ship R&D Ctr
ATTN: Code 2740
ATTN: Code 1740.5
ATTN: Code 177, E. Palmer
ATTN: Code 1700, W. Murray
ATTN: Code L42-3

Naval Civil Engrg Lab
ATTN: Code L51, R. Odello
ATTN: Code L51, S. Takahashi

Naval Facilities Engrg Cmd
ATTN: Code 04B

Naval Ocean Systems Center
ATTN: Code 013, E. Cooper
ATTN: Code 4471

Naval Postgraduate School
ATTN: Code 1424 Library

Naval Research Lab
ATTN: Code 8440, G. O'Hara
ATTN: Code 2627

Naval Sea Systems Cmd
ATTN: SEA-09G53

Naval Surface Weapons Ctr
ATTN: Code U401, M. Kleinerman
ATTN: Code R10
ATTN: Code R14
ATTN: Code F31

Naval Surface Weapons Ctr
ATTN: Tech Library & Info Svcs Br

DEPARTMENT OF THE NAVY (Continued)

Naval War College
ATTN: Code E-11, Tech Svcs

Naval Weapons Ctr
ATTN: Code 343, FKA6A2, Tech Svcs
ATTN: Code 266, C. Austin
ATTN: Code 3263, J. Bowen

Naval Weapons Evaluation Facility
ATTN: R. Hughes
ATTN: Code 10

Ofc of the Deputy Chief of Naval Ops
ATTN: NOP 981, U/SEA/ST WAR/NUC EN DEV
ATTN: OP 654C3, R. Piacesi

Office of Naval Rsch
ATTN: Code 474, N. Perrone

Strat Systems Project Ofc
ATTN: NSP-43

DEPARTMENT OF THE AIR FORCE

AFRCE-BMS/DEE
ATTN: DEB

Air Force Armament Lab
ATTN: DLYV, J. Collins

Air Force Geophysics Lab
ATTN: LWH, H. Ossing

Air Force Institute of Technology
ATTN: Library

Air Force Ofc of Scientific Rsch
ATTN: J. Allen
ATTN: B. Wolfson

Air Force Systems Cmd
ATTN: DLW

Air Force Weapons Lab
ATTN: NTES-G, S. Melzer
ATTN: NTE, M. Plamondon
ATTN: NTES-C, R. Henny
ATTN: SUL
ATTN: NTED

Ballistic Missile Office
ATTN: ENSN
ATTN: ENBF, D. Cace

Space Command
ATTN: XPX

Strategic Air Command
ATTN: XPFS
ATTN: NRI-STINFO Library

Civil Engrg Department
ATTN: W. Fluhr

DEPARTMENT OF ENERGY

Department of Energy
ATTN: CTID

DEPARTMENT OF ENERGY (Continued)

Department of Energy
ATTN: OMA/RD&T

Department of Energy
ATTN: Doc Con for Tech Library

OTHER GOVERNMENT AGENCIES

Department of the Interior
Bureau of Mines
ATTN: Tech Lib

Dept of The Interior, US Geological Surv
ATTN: D. Roddy

Federal Emergency Management Agency
ATTN: Hazard Eval & Vul Red Div

NASA
ATTN: R. Jackson

US Nuc Regulatory Commission
ATTN: R. Whipp for Div Sec, L. Shao

NATO

NATO School, SHAPE
ATTN: US Documents Officer

DEPARTMENT OF ENERGY CONTRACTORS

University of California
Lawrence Livermore National Lab
ATTN: Tech Info Dept Library

Oak Ridge National Lab
ATTN: Civil Def Res Proj
ATTN: Central Rsch Library

Sandia National Labs
ATTN: L. Vortman

DEPARTMENT OF DEFENSE CONTRACTORS

ACTA, Inc
ATTN: J. Collins

ACUREX Corp
ATTN: J. Stockton

Aerospace Corp
ATTN: L. Selzer
ATTN: P. Mathur
2 cy ATTN: Tech Info Svcs

Agbabian Associates
ATTN: M. Agbabian
ATTN: C. Bagge

Applied Research Associates, Inc
ATTN: H. Auld
ATTN: N. Higgins
ATTN: J. Bratton

Applied Theory, Inc
2 cy ATTN: J. Trulio

AVCO Systems Div
ATTN: Library A830

DEPARTMENT OF DEFENSE CONTRACTORS (Continued)

BDM Corp
ATTN: Corporate Library
ATTN: Lavagnino
ATTN: T. Neighbors

Bell Telephone Labs, Inc
ATTN: J. White

Boeing Aerospace Co
ATTN: M/S 42/37, K. Friddell
ATTN: M/S 13/13, R. Dyrdahl

Boeing Co
ATTN: J. Wooster
ATTN: Aerospace Library
ATTN: M/S 42/37, R. Carlson
ATTN: R. Holmes

California Institute of Technology
ATTN: T. Ahrens

California Research & Technology, Inc
ATTN: M. Rosenblatt
ATTN: Library
ATTN: K. Kreyenhagen

California Research & Technology, Inc
ATTN: D. Orphal

EG&G Wash Analytical Svcs Ctr, Inc
ATTN: Library

Electric Power Research Institute
ATTN: G. Sliter

Electro-Mech Systems, Inc
ATTN: R. Shunk

Franklin Institute
ATTN: Z. Zudans

General Dynamics Corp
ATTN: R. Dibrell

General Electric Co
ATTN: M. Bortner

General Research Corp
ATTN: K. Narasimhan
ATTN: TIO

Geo Centers, Inc
ATTN: E. Marram

H&H Consultants, Inc
ATTN: W. Hall
ATTN: J. Haltiwanger

H-Tech Labs, Inc
ATTN: B. Hartenbaum

IIT Research Institute
ATTN: Documents Library
ATTN: A. Longinow

Institute for Defense Analyses
ATTN: Classified Library
ATTN: Director

DEPARTMENT OF DEFENSE CONTRACTORS (Continued)

Kaman AviDyne
ATTN: N. Hobbs
ATTN: Library
ATTN: G. Zartarian
ATTN: R. Ruetenik

Kaman Sciences Corp
ATTN: F. Shelton
ATTN: Library

Kaman Tempo
ATTN: DASIAC

Kaman Tempo
ATTN: D. Sachs
ATTN: DASIAC

Karagozian & Case
ATTN: J. Karagozian

Lockheed Missiles & Space Co, Inc
ATTN: T. Geers

Management Science Associates
ATTN: K. Kaplan

Martin Marietta Corp
ATTN: A. Cowan
ATTN: G. Fotieo

Martin Marietta Denver Aerospace
ATTN: J. Donathan
ATTN: D-6074, G. Freyer

McDonnell Douglas Corp
ATTN: R. Halprin

Merritt CASES, Inc
ATTN: Library

Mitre Corp
ATTN: Director

University of New Mexico
ATTN: D. Calhoun
ATTN: N. Baum

University of New Mexico
ATTN: G. Triandafalidis

Nichols Research Corp, Inc
ATTN: N. Byrn
ATTN: W. Mendes

Pacific-Sierra Research Corp
ATTN: H. Brode, Chairman SAGE

Pacifica Technology
ATTN: R. Bjork
ATTN: G. Kent
ATTN: Tech Library

Physics Applications, Inc
ATTN: C. Vincent

Rand Corp
ATTN: Library
ATTN: P. Davis

DEPARTMENT OF DEFENSE CONTRACTORS (Continued)

Physics International Co
ATTN: J. Thomsen
ATTN: Tech Library
ATTN: F. Sauer

R&D Associates
ATTN: D. Simons
ATTN: Tech Info Ctr
ATTN: Dr. Chok Kau Lee
ATTN: J. Lewis
ATTN: P. Haas

S-CUBED
ATTN: K. Pyatt
ATTN: D. Grine
ATTN: Library
ATTN: T. Cherry

Science Applications, Inc
ATTN: Tech Library

Rand Corp
ATTN: B. Bennett

Science Applications, Inc
ATTN: R. Hoffmann

Science Applications, Inc
ATTN: W. Layson
ATTN: J. Cockayne
ATTN: G. Binninger

Southwest Research Institute
ATTN: W. Baker

DEPARTMENT OF DEFENSE CONTRACTORS (Continued)

SRI International
ATTN: G. Abrahamson

Teledyne Brown Engrg
ATTN: F. Leopard

Terra Tek, Inc
ATTN: A. Jones
ATTN: Library
ATTN: A. Abou-Sayed
ATTN: S. Green

Texas A&M University System
ATTN: H. Coyle

TRW Electronics & Defense Sector
ATTN: A. Feldman
ATTN: Tech Info Ctr
2 cy ATTN: N. Lipner

TRW Electronics & Defense Sector
ATTN: P. Dai
ATTN: G. Hulcher

Weidlinger Assoc, Consulting Engrg
ATTN: M. Baron
ATTN: J. McCormick
4 cy ATTN: J. Wright
4 cy ATTN: R. Smilowitz

Weidlinger Associates
ATTN: J. Isenberg

END

FILMED

3-84

DTIC